Scanning Microscopy

Volume 1 | Number 2 Article 41

2-9-1987

Vascular Changes in Popliteal Lymph Nodes due to Antigen Challenge in Normal and Lethally Irradiated Mice

Douglas A. Steeber
University of Wisconsin

Chris M. Erickson
University of Wisconsin

Kees C. Hodde
Amsterdam Medical Center

Ralph M. Albrecht
University of Wisconsin

Scanning Microscopy, Vol. 1, No. 2, 1987 (Pages 831-839)
Scanning Microscopy International, Chicago (AMF O'Hare), IL 60666 USA

0891-7035/87$3.00+.00

VASCULAR CHANGES IN POPLITEAL LYMPH NODES DUE TO ANTIGEN CHALLENGE IN NORMAL AND LETHALLY IRRADIATED MICE

Douglas A. Steeber, Chris M. Erickson, Kees C. Hodde[1], Ralph M. Albrecht*

Department of Veterinary Science
University of Wisconsin
Madison, Wisconsin 53706

[1] Amsterdam Medical Center
Lab. Exptl. Surgery
1105 AZ Amsterdam
Netherlands

(Received for publication August 13, 1986, and in revised form February 9, 1987)

Abstract

The microvascular system of the murine popliteal lymph node was investigated using scanning electron microscopy of microcorrosion casts. Time-dependent changes in the microvasculature following regional antigen challenge in normal and lymphocyte-depleted mice were studied. Normal lymph node microvasculature exhibited a significant increase in both the vascular bed and post-capillary venules containing high-endothelium in response to antigen challenge. Lymph nodes of lymphocyte-depleted mice showed no microvascular size increase following antigen challenge and a reduction in the amount of high-endothelium was observed.

Key Words: Lymph node, Blood vessels, High-endothelial venules, Corrosion casting, Irradiation.

*Address for correspondence:
R.M. Albrecht
Department of Veterinary Science
University of Wisconsin
1655 Linden Drive
Madison, Wisconsin 53706
Phone No.: (608) 263-4162

Introduction

The blood-vascular architecture of the peripheral lymph node has been the subject of research interest since the mid 1920s when Schulze (25) identified and described the unique endothelial morphology of the post-capillary venules (PCV). Since then numerous studies have been undertaken in an effort to describe and understand the complex microvasculature of the lymph node. The distribution and morphology of the microvasculature has been described using many techniques including light microscopy (4,19,21), electron microscopy (1,2,7,20), microangiography (18), and various histochemical techniques (14,23,26). Morphological changes in the lymph node microvascular system have been suggested to occur based on studies demonstrating alterations in blood flow (5,13,15), lymphocyte trafficking (3,10,12,14), and node weights (11,13,18) in response to various experimental conditions. Dispute concerning the nature of these microvascular changes still exists. The node microvascular system has previously been suggested to undergo endothelial cell proliferation during a primary immune response (5,13). Other findings indicate that a redistribution of the existing vasculature occurs rather than new vessel growth (15,17,18). Conflicting reports concerning the effects of experimental conditions on the high-endothelial (HE) cells of the PCV also exist. Several studies have shown pronounced morphological effects (e.g., flattening) in the HE cells in response to lymphocyte or antigen depletion (7,14,22), while others report no effects as a result of the same or similar treatments (28,29).

A three-dimensional study of the peripheral lymph node microvascular architecture is desirable in order to permit an accurate description of changes occurring during an immune response or as a result of other experimental conditions. In addition, this type of study allows an identification of the specific vessels involved and their relationship to one another, thus lending insight into the mechanisms of this vascular response. Techniques such as stereomicroangiography (16), alcian blue dye staining (1), and alpha-naphthylacetate esterase staining (23) have previously been used for three-dimensional viewing of the peripheral lymph node microvasculature with varying degrees of success. In this study we present a microcorrosion casting technique which can be applied to the study of lymphoid tissue microvasculature. This technique allows the three-dimensional visualization of the entire lymph node microvasculature through scanning electron microscopy

(SEM). Individual vessels, such as the high-endothelial venules (HEV), can be readily identified in the cast and their relationship to other vessels studied. Vascular changes occurring as a result of an immune response or experimental conditions can be assessed by this method. We have used microcorrosion casting to follow the vascular changes occurring in single lymph nodes following local antigen stimulation and to observe effects of lymphocyte depletion on the lymph node microvasculature.

Materials and Methods

Animals

Sixty male and female outbred Swiss mice (U.W. Charmany Farm, Madison, WI) between the ages of twelve and eighteen weeks were used in these studies.

Irradiation

Thirty of the above male and female mice received 800 rads total body irradiation from a Shepard Irradiator model 30 equipped with a ^{137}Ce source. The mice were irradiated with a single dose one day prior to footpad injections.

Cell Counts

Blood was collected from the tail veins of normal and irradiated mice and placed directly into 0.89% ammonium chloride (w/v in water). The samples were then stained with acridine orange and counted under UV illumination in a hemocytometer at 400X magnification.

Antigen Stimulation

At predetermined timepoints (0, 13 h, 2, 4, 7 days) prior to casting, the animals received footpad injections of both keyhole limpet hemocyanin (KLH) (CalBiochem, San Diego, CA) 43.0 mg/ml in sterile saline and 0.9% saline, filter sterilized through a 0.22 μm Millipore filter (Millipore Co., Bedford, MA). KLH (0.05 ml) was injected into the right rear footpad and an equal volume of sterile saline injected into the left rear footpad as a control.

Corrosion Casting

The methods used have been modified for use in mice from those previously described by Hodde and Nowell (19). Briefly, at the above time periods animals were anesthetized with an intramuscular injection of 0.15 ml Ketamine (100 mg/ml) supplemented with Rompun (0.25 mg/ml). The thoracic cavity was opened exposing the heart and 0.05 ml heparin (1000 U/ml) (Upjohn, Kalamazoo, MI) was immediately injected into the left ventricle and allowed to circulate. The left ventricle was punctured using an 18 ga needle and a polyethylene cannula (Intramedic PE 100) inserted into the aorta. The cannula was held in place with 5-0 silk tied around the aorta. A 20 cc polyethylene disposable syringe was filled with heparinized (10 U/ml), filter sterilized (0.22 μm Millipore) 0.9% saline warmed to 37°C. The syringe was attached to the cannula with an 18 ga needle. The right atrium was immediately opened to serve as an efferent port. The animal was perfused manually at a rate of 1-2 ml/min. The entire perfusion procedure was carried out under a heat lamp to prevent either the animal or perfusate from cooling. At the end of the perfusion period the animal was moved under a fume hood for casting. Equal volumes of Mercox resin (Ladd, Burlington, VT) and methylmethacrylate monomer, containing 0.16 g/ml catalyst, were drawn into a 10 cc syringe and mixed by gentle inversion. The syringe was attached to the cannula and the resin perfused manually at a rate of 1-2 ml/min. The animal was then placed in a plastic bag and polymerization allowed to occur in a 60°C water bath for 2 h. The popliteal lymph nodes were dissected out, placed in vials containing distilled water and kept at 50°C for two days. Next, the tissue was macerated in a 20% NaOH solution at 50°C for four days with frequent changes of solution. The casts were then placed in a 5.0% detergent solution for one day and finally were thoroughly rinsed several times in distilled, deionized water.

SEM Preparation

Casts were dehydrated in 100% sieve dried ethanol and dried by the critical point method using liquid CO_2 as the transitional fluid. The casts were mounted on stubs with silver paint, sputter coated with 10 nm gold palladium and viewed with a JEOL JSM-35C scanning electron microscope at 10 kV accelerating voltage.

Results

Microvascular changes which occur during a primary immune response to keyhole limpet hemocyanin (KLH) are demonstrated in Figures 1, 2, and 3. Figures 1a and 1b are microcorrosion casts of a control and a KLH stimulated popliteal lymph node pair, respectively. Casting was performed 13 h after sterile saline injection in the control (left footpad) side (Figure 1a) and KLH injection in the challenged (right footpad) side (Figure 1b). At this time no size increase is seen in the microvascular system of the stimulated node. In the control node a well formed thin peripheral (subcapsular) capillary network is seen above and surrounding several high-endothelial venules (HEV). In the contralateral stimulated node this capillary network appears less extensive, due in part to the angle of the micrograph, while the HEV remain morphologically similar to the control. At four days post-challenge a marked size increase is observed in the microvascular system of the stimulated node (compare Figures 2a and 2b). This size increase corresponds to an approximate four-fold volume increase over the control node. The peripheral capillary network is minimal; however, extensive capillary networks are now present in the cortex and medulla between the HEV of the stimulated node. The contralateral control node exhibits typical vascular morphology of an unstimulated node (compare Figures 2a and 1a). At seven days post-challenge the microvascular system of the stimulated node increases slightly to approximately four-and one-half times the volume of the contralateral control node (compare Figures 3a and 3b). At this time a peripheral capillary network is evident above and surrounding the HEV in the stimulated node. The control node shows no size increase relative to other controls (Figures 1a and 2a) but does appear to show some loss of the peripheral capillary network.

The ability to identify the individual vessels and to determine their interrelationships with one another is illustrated in Figure 4. In this stereomicrograph the blood flow from arteriole to connecting capillary to HEV can easily be followed. The ability to identify and follow individual vessels, such as the HEV, is demonstrated in Figures 5a and 5b. In Figure 5a a HEV is demonstrated beginning abruptly at the efferent end of a connecting capillary. In Figure 5b the end of the HEV can be demonstrated by the gradual replacement of typical high-endothelial (HE) cell impressions with those of the normal flat-endothelial cells characteristic of a draining vein. The small "plaques" that are seen at the base of the HE cell impressions may be related to sites

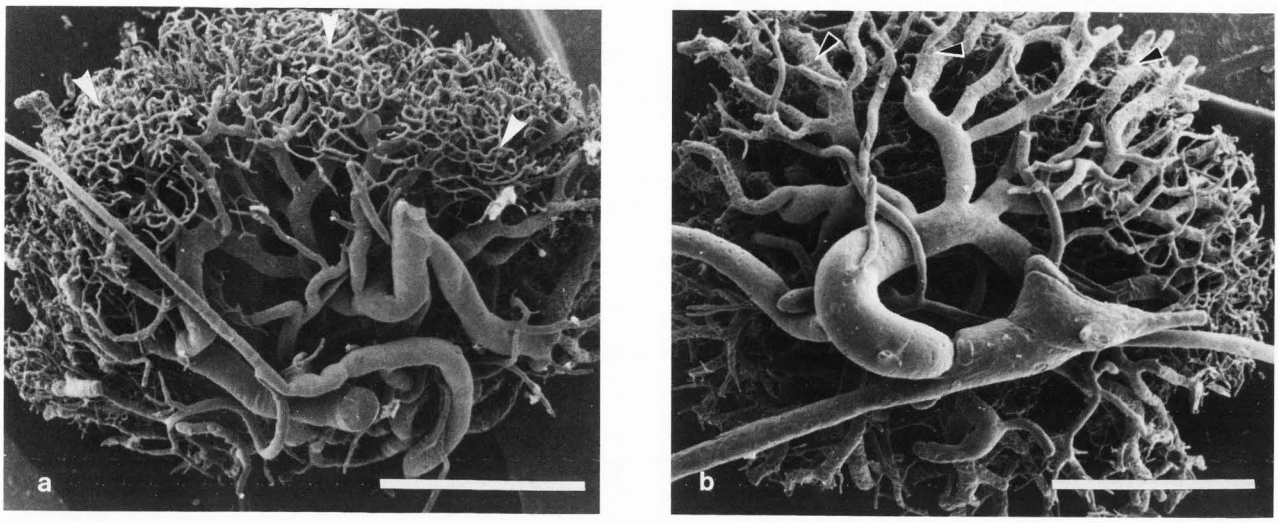

Figure 1 Vascular corrosion casts of a mouse popliteal lymph node pair 13 h following footpad inoculations. (a) Saline injection. Note thin "layer" of peripheral capillary network (arrowheads). Bar = 0.5 mm. (b) KLH injection. Typical high-endothelial venules (arrowheads) can be clearly seen. Bar = 0.5 mm.

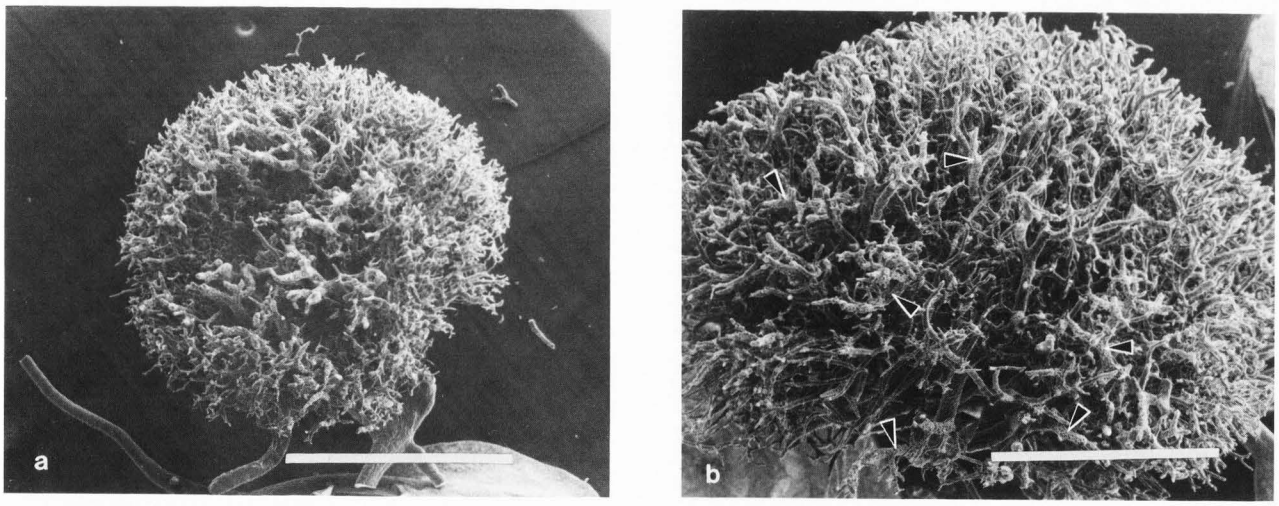

Figure 2 Popliteal lymph node pair four days following footpad inoculations. (a) Saline injection. Bar = 1 mm. (b) KLH injection. Many high-endothelial venules (arrowheads) are readily apparent. Bar = 1 mm.

of lymphocyte attachment. These "plaques" are never associated with any other vessel type (e.g., arteries, capillaries) or with the HEV of lymphocyte-depleted animals.

The morphology of the HEV was observed to remain unchanged during a primary immune response to KLH as shown in Figures 5a and 5c. Figure 5a shows typical HE cell impressions of the HEV seen in the cast of a stimulated lymph node. The HE cells leave a deep and generally regular pattern of impressions which covers the entire surface of the cast. The HEV are seen to be fed directly from capillaries and begin abruptly as demonstrated by the rapid increase in vessel diameter and deep HE cell impressions. Figure 5c demonstrates the same HE cell imprint morphology in the cast of the contralateral control node. In contrast, the impressions of the HE cells in the lymphocyte-depleted animals were observed to be much shallower than those seen in the casts of normal animals (compare Figures 6a and 6b with Figures 5a and 5c). Shallower HE cell impressions were observed by day five post-irradiation (Figure 6a) at which time the peripheral WBC counts were reduced more than 95%, and still evident at day eight post-irradiation (Figure 6b) when the WBC count was reduced nearly 98% compared to controls.

Figures 7 and 8 illustrate the microvascular changes occurring in lymphocyte-depleted animals during a primary immune response to KLH. Figure 7a shows a control popliteal node four days post-saline injection and five days post-irradiation. The peripheral capillary network is absent and the HEV exhibit shallow HE cell impressions. Figure 7b is the contralateral stimulated node. The peripheral capillary network is absent and the normal microvascular size increase,

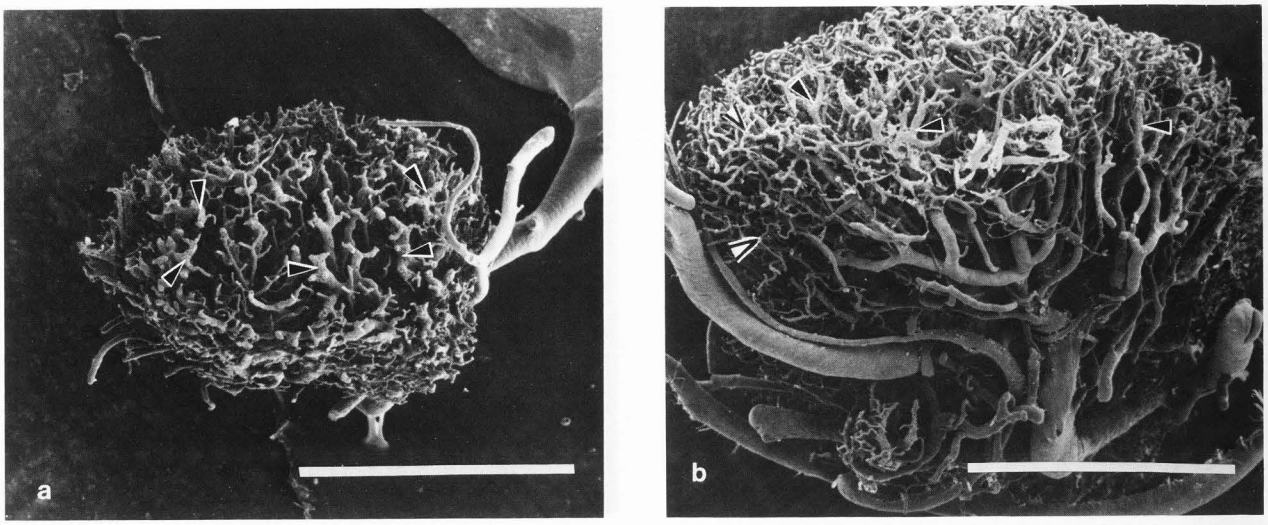

Figure 3 Popliteal lymph node pair seven days following footpad inoculations. (a) Saline injection. High-endothelial venules are distinctly visible (arrowheads). Bar = 1 mm. (b) KLH injection. The peripheral capillary network (white arrowheads) and high-endothelial venules (bordered arrowheads) are visible. Bar = 1 mm.

resulting from antigen stimulation in non-lymphocyte-depleted animals, does not occur (compare Figures 7a and 7b with Figures 2a and 2b). In fact, the dimensions of this irradiated, stimulated node are comparable to control nodes of normal animals (Figures 1a, 2a, and 3a). Figures 8a and 8b illustrate the lack of size increase in the stimulated node over the contralateral control node at seven days post-challenge and eight days post-irradiation. The HE cell impressions are again observed to be shallower than those seen in casts of normal animals (compare to Figure 5a).

Discussion

The microvascular system of the peripheral lymph node has been suggested to undergo significant alterations, including increased blood flow and vascularity, during an immune response to antigen (3,5,13,15,18). The mechanism(s) by which these alterations occur following antigen stimulation is still unresolved. Herman et al. (18) reported these increases in blood flow and vascularity to be the result of a redistribution and straightening of the existing vessels. Others (5,13) have suggested that the increased blood flow is due to vascular dilation and the increased vascularity due to new vessel growth. Our results support an initial period of vascular dilation and redistribution of blood flow followed by a period of vascular proliferation in response to antigen stimulation.

The initial redistribution of blood flow was observed 13 h post-antigen stimulation. This corresponds very closely with peaks in blood flow observed at approximately 14 h following antigen stimulation (13). At this time the peripheral capillary network appeared to be less extensive in the stimulated nodes than in the control nodes (see Figure 1). This apparent alteration in resin flow may be the result of a diversion of the blood flow through arterio-venous anastomoses (AVA). The presence of AVA in the peripheral lymph node has been reported previously (1,5,15,20) and an increase in shunt flow following antigen stimulation has been described by Herman et al. (17). We have not been able to confirm the presence of AVA in our casts and further study is warranted to clarify this point.

Microvascular size increases were first observed at day two post-antigen stimulation (data not shown) and peaked at day seven. At day seven post-antigen stimulation the microvascular volume increased four- and one-half-fold relative to its contralateral saline injected control. To achieve such a size increase by vessel redistribution and expansion without new vessel growth, as argued by Herman et al. (18), a corresponding reduction in the vascular density, due to spreading and straightening of vessels as the bed expands to fill the increased volume, should be observed. Our results show that the volume increase occurs in a stimulated node concurrent with a significant increase in the vascular density (see Figure 3). This could be explained by assuming the existence of a reserve of preformed "collapsed" vessels which become filled following antigen stimulation. While such collapsed vessels could be contained within the unstimulated node they would occupy a considerable area, most probably in the subcapsular region. At present no such reserve has been reported. Therefore, we feel vessel growth accounts, in part, for the increases in both vascular size and density observed following antigen stimulation.

The high-endothelial venules (HEV) found in the peripheral lymphoid tissue have been intensely studied since Gowans and Knight (8) demonstrated their involvement in lymphocyte trafficking. To study the activity of these specialized venules and determine their interactions with other vessels, researchers have attempted to find a suitable means of constructing a three-dimensional picture of the entire peripheral lymph node microvasculature (1,2,23). Previously the ability to completely and accurately replicate the microvascular system of lymphoid tissues by microcorrosion casting was demonstrated (20). In the present study microcorrosion casting was found to be a simple and direct way of identifying and viewing the individual vessels of the peripheral lymph node. This technique allowed unobstructed three-dimensional viewing of all the vessels in the peripheral lymph node

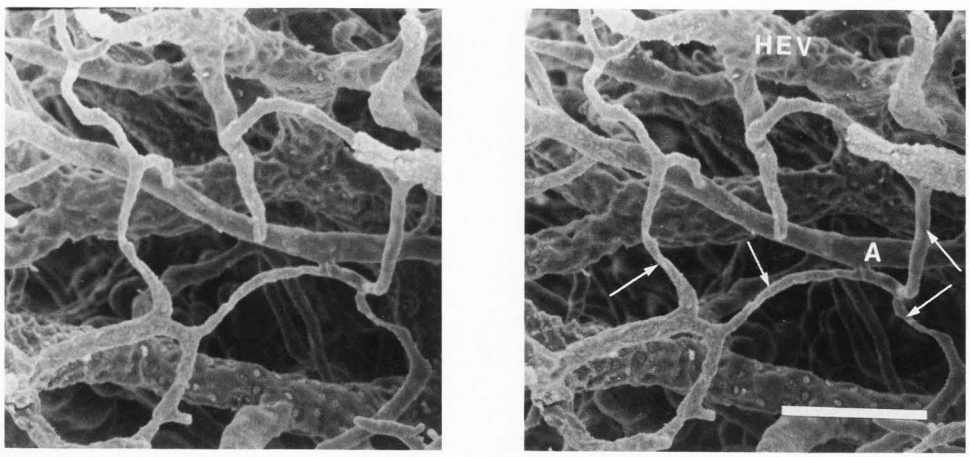

Figure 4 Stereomicrograph of the peripheral aspects of a popliteal lymph node cast. Blood flow can be followed from arteriole (A) to high-endothelial venule (HEV). Arrows point to connecting capillaries. Bar = 100 μm.

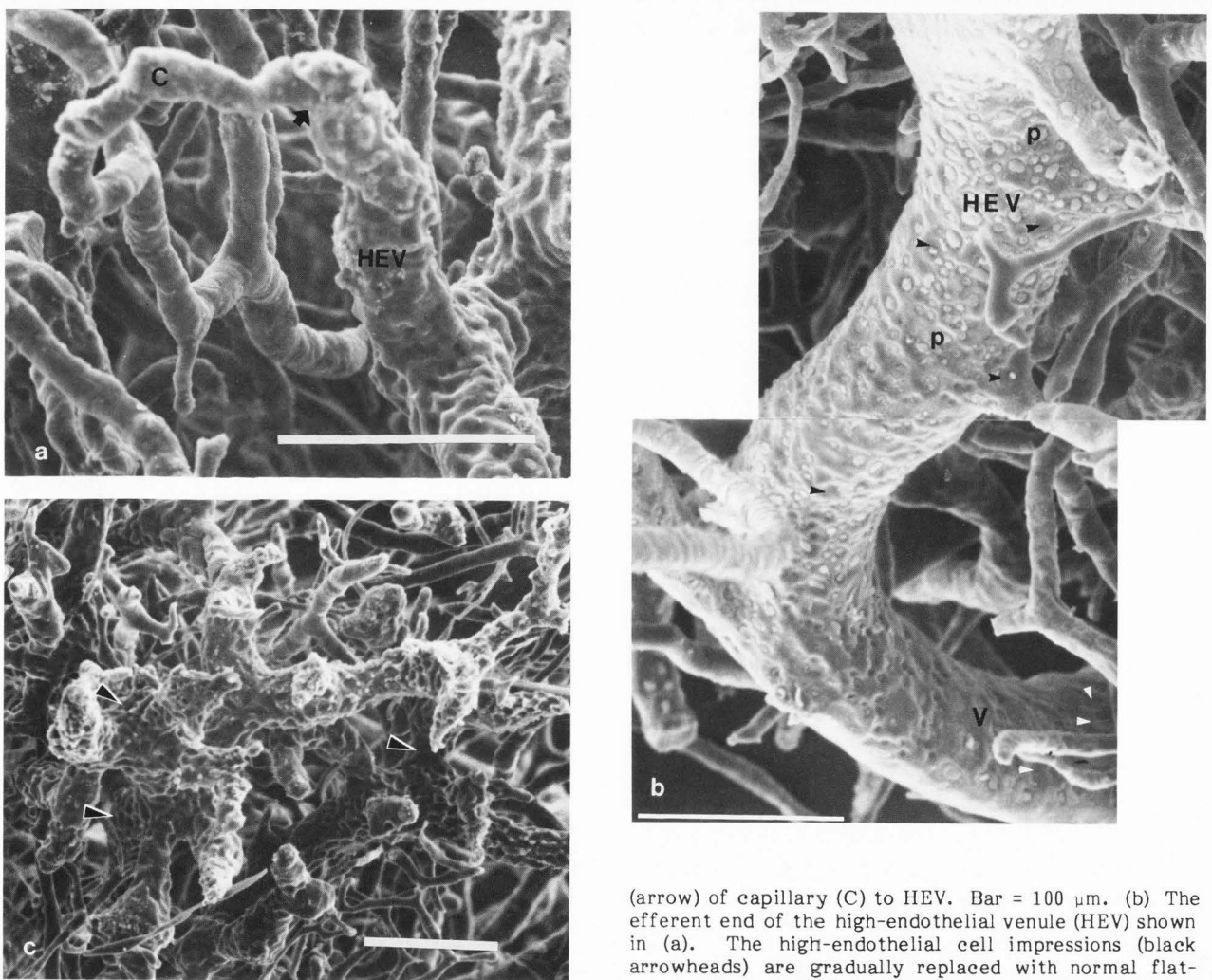

Figure 5 Micrographs taken from a popliteal lymph node pair three days following footpad inoculations. (a) KLH injection. The efferent end of a capillary is seen to connect directly to the afferent end of a high-endothelial venule (HEV). Note the abrupt transition (arrow) of capillary (C) to HEV. Bar = 100 μm. (b) The efferent end of the high-endothelial venule (HEV) shown in (a). The high-endothelial cell impressions (black arrowheads) are gradually replaced with normal flat-endothelial cell (white arrowheads) impressions of a draining vein (V). Small plaques (p) at the base of the high-endothelial cell impressions can be seen. Bar = 100 μm. (c) Saline injection. Note the imprint morphology of the high-endothelial venules (arrowheads) is similar to that seen in the stimulated node (a). Bar = 100 μm.

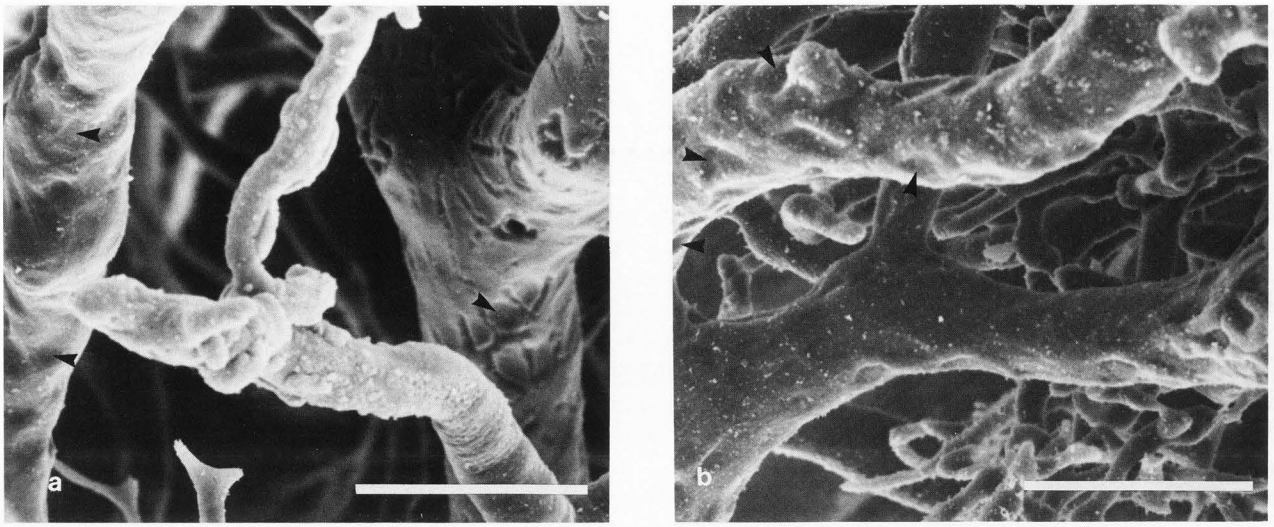

Figure 6 High-endothelial venules of popliteal lymph nodes. (a) Four days following KLH footpad injection and 800 rads irradiation (one day prior to injection). Note the impression morphology of the high-endothelial cells (arrowheads). Bar = 50 μm. (b) Seven days following saline footpad injection and 800 rads irradiation (one day prior to injection). Note the morphology of the high-endothelial cell impressions (arrowheads). Bar = 50 μm.

which could not have been accomplished using two-dimensional photographic or radiographic techniques. The individual vessels were readily identified in the casts by their diameter, location, and distinctive endothelial surface morphology as previously described by Hodde and Nowell (19).

The ability to identify HEV in corrosion casts by their distinctive cuboidal endothelial cell morphology has previously been described by Yamaguchi and Schoefl (29) in the peyer's patch, but to our knowledge has not been reported in other peripheral lymphoid tissues. The HEV were particularly easy to identify and trace because of this unique endothelial cell morphology. The high-endothelial (HE) cell impressions were only observed in the casts on some post-capillary venules, were never seen in conjunction with arteries, capillaries, or large veins, and were located between the capillaries of the cortex and large draining veins in the hilar region as previously described (1,2,18,20,21,23). Capillaries in the cortex and medulla were seen to drain directly into HEV (see Figure 5a) in contrast to the observations of Anderson and Anderson (1) who reported that capillaries first drain into venules lined by low-endothelium which then drain into HEV.

Following antigen stimulation, Herman (15) reported observing an increase of high-endothelium on side branches of post-capillary venules (PCV). Prior to antigen challenge these venules had been lined only by low endothelium (LEV). These observations led Herman to conclude that development of HEV from LEV in side branches of PCV was a major source of new HEV in stimulated nodes. Our findings also indicate that a significant increase in HEV occurs, although growth of new HEV, rather than conversion of LEV to HEV, appeared to account for the major increase in new HEV. We also found the morphology and general distribution of the HEV, relative to the overall shape of the node, to remain constant throughout a primary immune response to KLH. In addition, the increase in the amount of microvasculature lined by high-endothelium appears to be in proportion to the size increase of the stimulated node. Therefore, the approximate four-and one-half-fold increase in microvascular volume observed in the stimulated node results in a corresponding increase in the amount of HEV.

Effects of lymphocyte depletion on the morphology of the HEV in the peripheral lymph node have been reported. Goldschneider and McGregor (7) reported that lymphocyte-depleted animals showed a dilation and subsequent loss of cytoplasm in the high-endothelial (HE) cells. This finding was later confirmed by Miller (22) and Hendriks and Eestermans (14). Others (4,29) have observed the HE cells to remain unchanged in response to similar lymphocyte depletion studies. Our results indicate that a morphological change in the HE cells does occur in response to lymphocyte depletion. HE cell impressions were observed to become shallower than those typically seen in casts of non-lymphocyte-depleted animals. These shallower HE cell impressions are believed to be the result of a corresponding "flattening" of the HE cells lining the HEV in lymphocyte-depleted animals. Also, the initial shunting of flow occurred but the normal microvascular size increase seen in casts of non-lymphocyte-depleted animals, in response to antigen stimulation, was absent (Figures 7 and 8).

The possibility that our results could, in part, be due to direct radiation damage of the endothelium itself and not a result of lymphocyte depletion has been considered. To lessen any potential radiation effects on the endothelial cells, antigen stimulation was performed after irradiation so these endothelial cells would be in a less activated state and thus more radioresistant. Possible radiation effects on the peripheral lymph node have been reported previously (9,27). Ross et al. (24) found that LD_{50} levels of irradiation produced no direct damage to the lymph node endothelium. More recently, Fromer and Klintworth (6) demonstrated that endothelial cell proliferation could still occur after receiving radiation doses as high as 2100 rads which is nearly three times the dose received by mice in the present study.

Microcorrosion casting was found to be a very

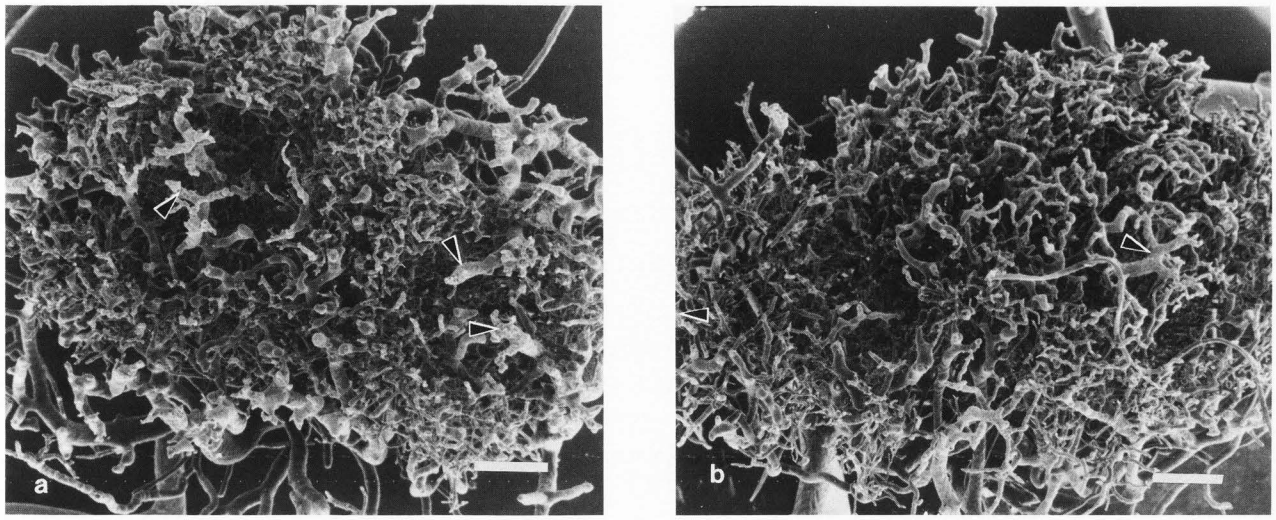

Figure 7 Popliteal lymph node pair four days following footpad inoculations and 800 rads irradiation (one day prior to injection). (a) Saline injection. High-endothelial venules are visible (arrowheads). Bar = 200 μm. (b) KLH injection. High-endothelial venules are visible (arrowheads). Bar = 200 μm.

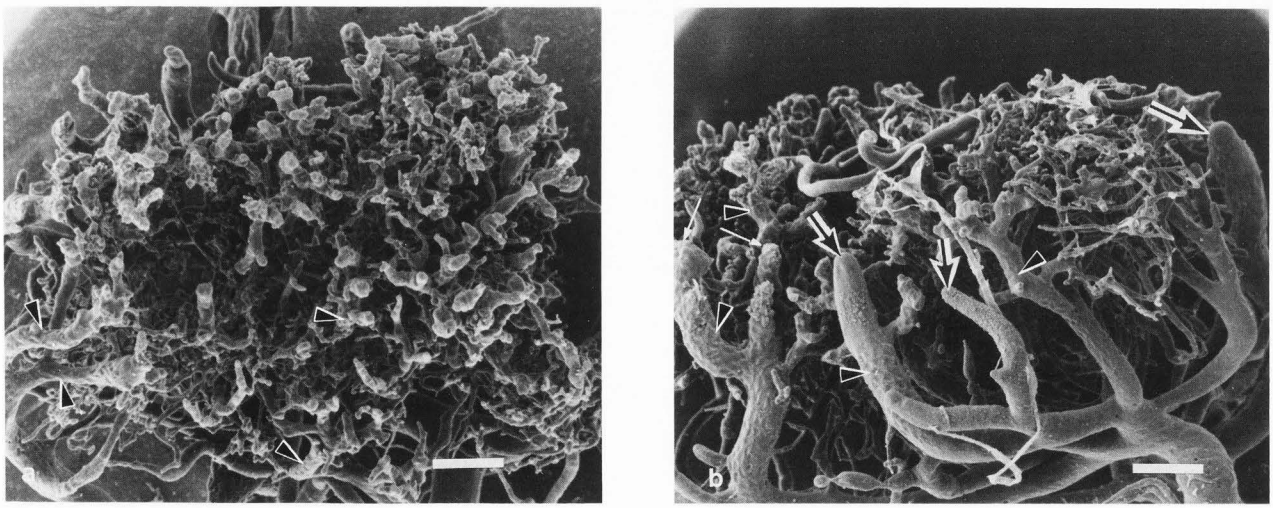

Figure 8 Popliteal lymph node pair seven days following footpad inoculations and 800 rads irradiation (one day prior to injection). (a) Saline injection. Note high-endothelial venules are visible (arrowheads). Bar = 100 μm. (b) KLH injection. High-endothelial venules are visible (arrowheads). Several of the blind ends (black arrows) are due to incomplete filling of resin while others (white arrows) appear to be "true" blind ends in which the vessel itself has ended, as evidenced by the continuous impressions of the endothelium in the cast. Bar = 100 μm.

direct means of studying individual vessel interactions and their response to both antigen challenge and lymphocyte depletion in the peripheral lymph node. This technique would prove very useful in investigations concerning the effects of various experimental regimes, such as chemotherapy, on the microvasculature of primary and secondary lymphoid tissues.

Acknowledgments

The authors wish to thank L. Sam, A.J. Rynders, and S.A. Kleman for the early development of the casting technique. We also thank R.L. Hoffman and J.A. Oliver for their technical assistance.

References

1. Anderson AO, Anderson ND. (1975). Studies on the structure and permeability of the microvasculature in normal rat lymph nodes. Amer. J. Path. 80, 387-418.

2. Belisle C, Sainte-Marie G. (1981). Tridimensional study of the deep cortex of the rat lymph node. III. Morphology of the deep cortex units. Anat. Rec.199, 213-226.

3. Cahill RNP, Frost H, Trnka Z. (1976). The effects of antigen on the migration of recirculating lymphocytes through single lymph nodes. J. Exp. Med. 143, 870-888.

4. Claesson MH, Jorgensen O, Ropke C. (1971). Light and electron microscopic studies of the paracortical post-capillary high-endothelial venules. Z. Zellforsch. 119, 195-207.
5. Davidson JW, Hobbs BB, Fletch AL. (1973). The microcirculatory unit of the mammalian lymph node. Bibl. Anat. 11, 423-427.
6. Fromer CH, Klintworth GK. (1975). An evaluation of the role of leukocytes in the pathogenesis of experimentally induced corneal vascularization. Amer. J. Path. 81, 531-544.
7. Goldschneider I, McGregor DD. (1968). Migration of lymphocytes and thymocytes in the rat. I. The route of migration from blood to spleen and lymph nodes. J. Exp. Med. 127, 155-168.
8. Gowans JL, Knight EJ. (1964). The route of recirculation of lymphocytes in the rat. Proc. Roy. Soc. Ser. B. 159, 257-282.
9. Hall JG, Morris B. (1964). Effect of x-irradiation of the popliteal lymph-node on its output of lymphocytes and immunological responsiveness. Lancet. 1, 1077-1080.
10. Hall JG, Morris B. (1965). The origin of the cells in the efferent lymph from a single lymph node. J. Exp. Med. 121, 901-910.
11. Hall JG, Morris B, Moreno GD, Bessis MC. (1967). The ultrastructure and function of the cells in lymph following antigenic stimulation. J. Exp. Med. 125, 91-110.
12. Hay JB, Cahill RNP, Trnka Z. (1974). The kinetics of antigen-reactive cells during lymphocyte recruitment. Cell. Immunol.10, 145-153.
13. Hay JB, Hobbs BB. (1977). The flow of blood to lymph nodes and its relation to lymphocyte traffic and the immune response. J. Exp. Med. 145, 31-44.
14. Hendriks HR, Eestermans IL. (1983). Disappearance and reappearance of high endothelial venules and immigrating lymphocytes in lymph nodes deprived of afferent lymphatic vessels: a possible regulatory role of macrophages in lymphocyte migration. Eur. J. Immunol. 13, 663-669.
15. Herman PG. (1980). Microcirculation of organized lymphoid tissues. Monogr. Allergy. 16, 126-142.
16. Herman PG, Ohba S, Mellins HZ. (1969). Blood microcirculation in the lymph node. Radiology. 92, 1073-1080.
17. Herman PG, Utsunomiya R, Hessel J. (1979). Arteriovenous shunting in the lymph node before and after antigenic stimulus. Immunology. 36, 793-797.
18. Herman PG, Yamamoto I, Mellins HZ. (1972). Blood microcirculation in the lymph node during the primary immune response. J. Exp. Med. 136, 697-714.
19. Hodde KC, Nowell JA. (1980). SEM of microcorrosion casts. Scanning Electron Microsc. 1980; II: 89-106.
20. Irino S, Takasugi N, Murakami T. (1981). Vascular architecture of thymus and lymph nodes: Blood vessels, transmural passage of lymphocytes, and cell-interactions. Scanning Electron Microsc. 1981; III: 89-98.
21. Mikata A, Niki R, Watanabe S. (1968). Reticuloendothelial system of the lymph node parenchyma, with special reference to post-capillary venules and granuloma formation. Recent Adv. RES. Res. 8, 143-154.
22. Miller JJ. (1969). Studies of the phylogeny and ontogeny of the specialized lymphatic tissue venules. Lab. Invest. 21, 484-490.
23. Muller E, Stempfel S. (1985). A three-dimensional reconstruction of high endothelial venules in the mouse lymph node: an enzyme-histochemical study. Anat. Rec. 212, 424-429.
24. Ross MH, Furth J, Bigelow RR. (1952). Changes in cellular composition of the lymph caused by ionizing radiations. Blood. 7, 417-428.
25. Schulze W. (1925). Untersuchungen uber die kapillaren und postkapillaren venen des lymphatischer organe. Ztschr. f. Anat. 76, 421-462.
26. Smith C, Henon BK. (1959). Histological and histochemical study of high endothelium of post capillary veins of the lymph node. Anat. Rec. 135, 207-211.
27. Smith C, Wharton TJ, Gerhardt AM. (1958). Studies on the thymus of the mammal. XI. Histochemical studies of thymus, spleen, and lymph node in normal and irradiated mice. Anat. Rec. 131, 369-387.
28. van Deurs B, Ropke C. (1975). The postnatal development of high-endothelial venules in lymph nodes of mice. Anat. Rec. 181, 659-678.
29. Yamaguchi K, Schoefl GI. (1983). Blood vessels of the peyer's patch in the mouse: III. High-endothelium venules. Anat. Rec. 206, 419-438.

Discussion with Reviewers

J. Walmsley: Does the volume increase at a constant rate over the 7 day period or do you see a plateau early after which only a minor size increase is seen?
Authors: In general, we see a plateau at day 4 post-challenge followed by slight size increases in the microvasculature over the next few days. The plateau may occur slightly earlier or later due to individual differences in the animals.

J. Walmsley: Since no direct endothelial damage is seen due to irradiation, what is the explanation for the similar morphology of the HEV from control and stimulated irradiated nodes?
Authors: We feel the most likely explanation for this occurrence is the decrease in circulating levels of lymphocytes following irradiation. We have found the morphological changes in the HEV to correspond to the decreasing levels of lymphocytes. If lymphocyte trafficking is, in part, responsible for the maintenance of the high cuboidal morphology of the HE cells, then a depletion of lymphocytes would be expected to affect HE cells in both stimulated and unstimulated nodes since trafficking occurs, to some extent, in both. However, at this time we have no direct evidence to support such a relationship.

F.E. Hossler: You refer to "peripheral capillary bed" and also to cortex. By definition the cortex is the peripheral zone of the lymph node (except at the hilus). Could you describe more exactly where the peripheral capillary bed is located?
Authors: In our description we use "peripheral" to indicate the location of the capillary network in relation to the cast. Since this network is located above the high-endothelial-venules, which are found in the paracortical region, this network is most likely located in the outer cortex in the subcapsular area.

A. Castenholz: In the legend of Figure 5b you mention that the small "plaques" appearing at the base of the

cell impressions of a HEV cast could be related to the sites of lymphocyte attachment. If that would be the explanation for this phenomenon, the location of the cells would not correspond to the cells seen in common tissue preparations perfused under normal conditions. In our tissue preparations of lymph node tissue and also in the micrographs recently published by Yechun He (Arch. Histol. Jap. 48, 1-15,(1985)) the cells obviously partly adhering to, partly passing through the high endothelium are located in the intercellular gaps rather than on the bulging central part of the endothelial cells. In your cast, however, the bulging parts correspond to the impressions and are occupied by the "plaques" while the crest-like protruding structures in your cast do not exhibit such a phenomenon.

Authors: At this time we feel these "plaques" may be associated with lymphocyte attachment based on several observations. First, these "plaques" are only seen associated with HEV, where lymphocyte attachment and trafficking are known to occur, and never in casts of other vessel types. Second, we observe the presence of many more "plaques" associated with the HEV of stimulated nodes (high level of lymphocyte trafficking) than in unstimulated nodes (low level of lymphocyte trafficking). Third, we have never observed these "plaques" associated with the HEV of nodes from irradiated animals in which the numbers of circulating lymphocytes available for trafficking are significantly reduced.

While we feel these "plaques" may be related to lymphocyte attachment, we do not believe that this must also represent the site of lymphocyte transit across the endothelium. It has been shown that lymphocytes recognize and bind specific surface receptors on the high-endothelial cells before they transverse the endothelium (Gallatin WM, Weissman IL, Butcher EC. (1983). Nature, 304, 30-34.). We believe the "plaques" are a result of lymphocytes binding at these receptor sites and that they may then migrate to specific areas (e.g., intercellular gaps) to transverse the endothelial wall.

A. Castenholz: Why does a structural element which must virtually cause an additional impression in the resin produce a positive "plaque"?

Authors: We believe that the "plaques" are formed as a result of lymphocytes binding to endothelial cells rather than by a "lymphocyte-binding structural element". For a positive "plaque" to be produced the lymphocyte must cause a slight invagination of the endothelial cell surface upon binding. Therefore, when the resin flows into a HEV it displaces the lymphocytes and fills in the invaginations producing positive "plaques" in the endothelial cell impressions.

F.E. Hossler: We have been testing several low viscosity resins and resin combinations for suitability as casting media. Presumably your addition of methylmethacrylate monomer to Mercox reduces resin viscosity. What is the viscosity of the mixture compared to Mercox?

Authors: Ladd reports the viscosity of Mercox to be in the range of 20-30 cps. The viscosity of our resin was 31 cps. The viscosity of the methylmethacrylate monomer is 0.5 cps. The viscosity of the 1:1 mixture (v:v) is 3.1 cps.

F.E. Hossler: What effect does this addition have on polymerization time, durability of the cast in the electron beam and during handling?

Authors: The addition of monomer significantly lengthens the polymerization time of the resin. In our hands the undiluted Mercox has a polymerization time of 6-8 minutes while the Mercox-monomer mixture has a polymerization time of 17-20 minutes. We have not found the durability of the casts in the electron beam to be reduced at the low kV used (10 kV) or in handling the casts during preparation.

F.E. Hossler: What is the source of the monomer and are there any particular purity requirements?

Authors: We obtain our methylmethacrylate monomer from an on-campus source. It is readily obtainable from a number of commercial sources (e.g., Aldrich). Our monomer is 99% pure and is inhibited with 10 ppm hydroquinone monomethyl ether. We are unaware of any other purity requirements.

F.E. Hossler: Presumably the detergent rinse following maceration helps remove lipids. Which detergent do you prefer?

Authors: We have obtained very good results using Contrad 70 (American Scientific Products, McGaw Park, IL).